Supplementary Information

A programmable bispecific nano-immuno-engager promotes T cell homing and reprograms tumour microenvironment

Lu Zhang[1,2,*], Ruonan Bo[1], Yi Wu[1], Longmeng Li[1], Zheng Zhu[1], Ai-Hong Ma[1], Wenwu Xiao[1], Yanyu Huang[1], Tatu Rojalin[1], Xingbin Yin[1], Yongheng Wang[1], Hongyong Zhang[1], Kelmen E. Low[1], Kiana Lee[1], Yousif Ajena[1], Di Jing[1], Dalin Zhang[1], Christopher M. Baehr[1], Ruiwu Liu[1], Lei Wang[3,*], Yuanpei Li[1,*] and Kit S. Lam[1,4,*]

[1]Department of Biochemistry and Molecular Medicine, UC Davis NCI-designated Comprehensive Cancer Center, University of California Davis, Sacramento, CA, USA.
[2]Department of Biomedical Engineering, Southern University of Science and Technology, Shenzhen, Guangdong, China.
[3]CAS Center for Excellence in Nanoscience, CAS Key Laboratory for Biomedical Effects of Nanomaterials and Nanosafety, National Center for Nanoscience and Technology, Beijing, China.
[4]Division of Hematology and Oncology, Department of Internal Medicine, School of Medicine, University of California Davis, Sacramento, CA, USA.

*e-mail: kslam@ucdavis.edu; zhanglu@sustech.edu.cn; lypli@ucdavis.edu; wanglei@nanoctr.cn.

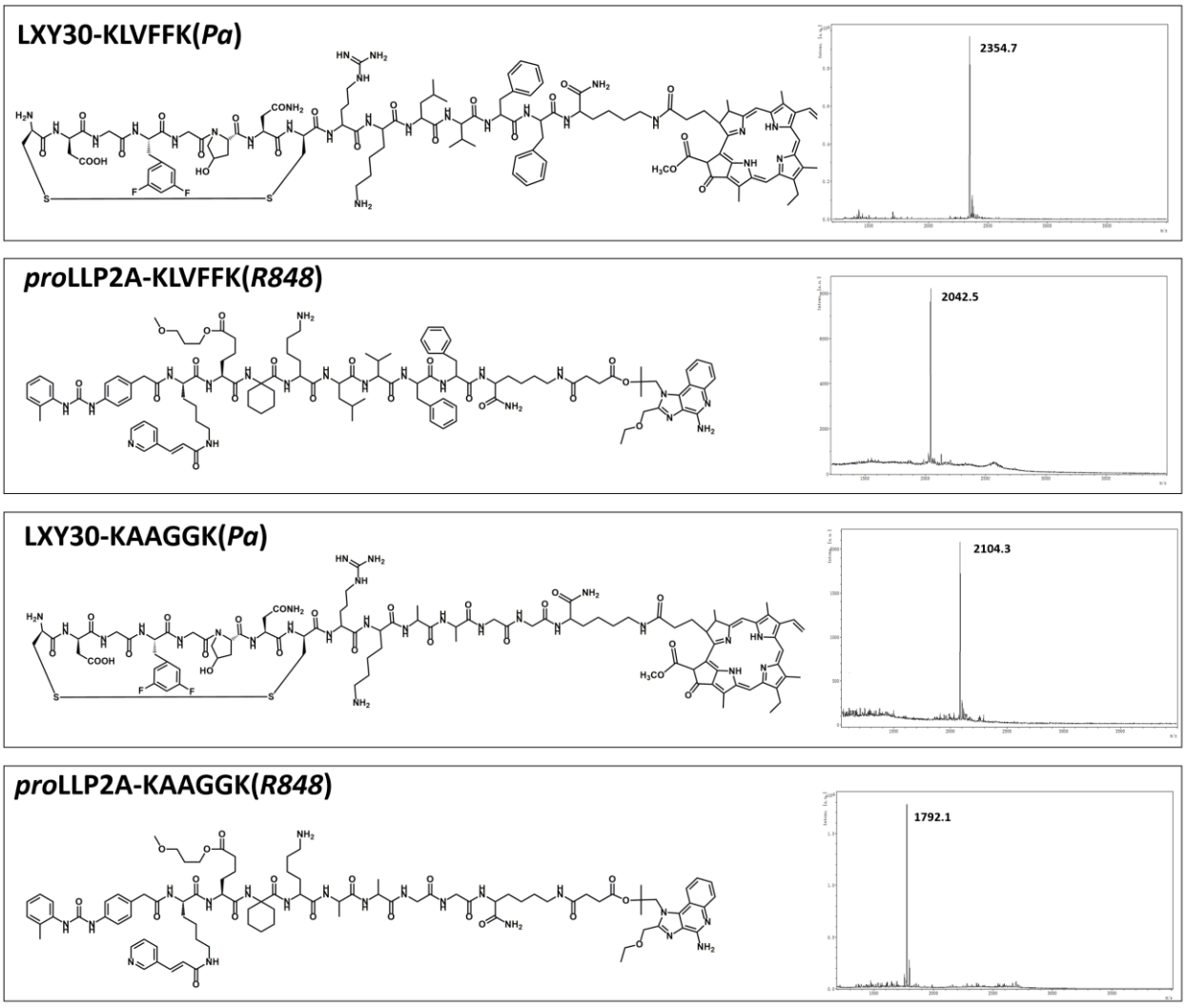

Supplementary Fig. 1. Chemical structure and mass spectra *via* MALDI-TOF of transformable peptide monomer: TPM1 LXY30-KLVFFK(*Pa*), TPM2 *pro*LLP2A-KLVFFK(*R848*), CTPM3 LXY30-KAAGGK(*Pa*), CTPM4 *pro*LLP2A-KAAGGK(*R848*). Experiments were repeated three times.

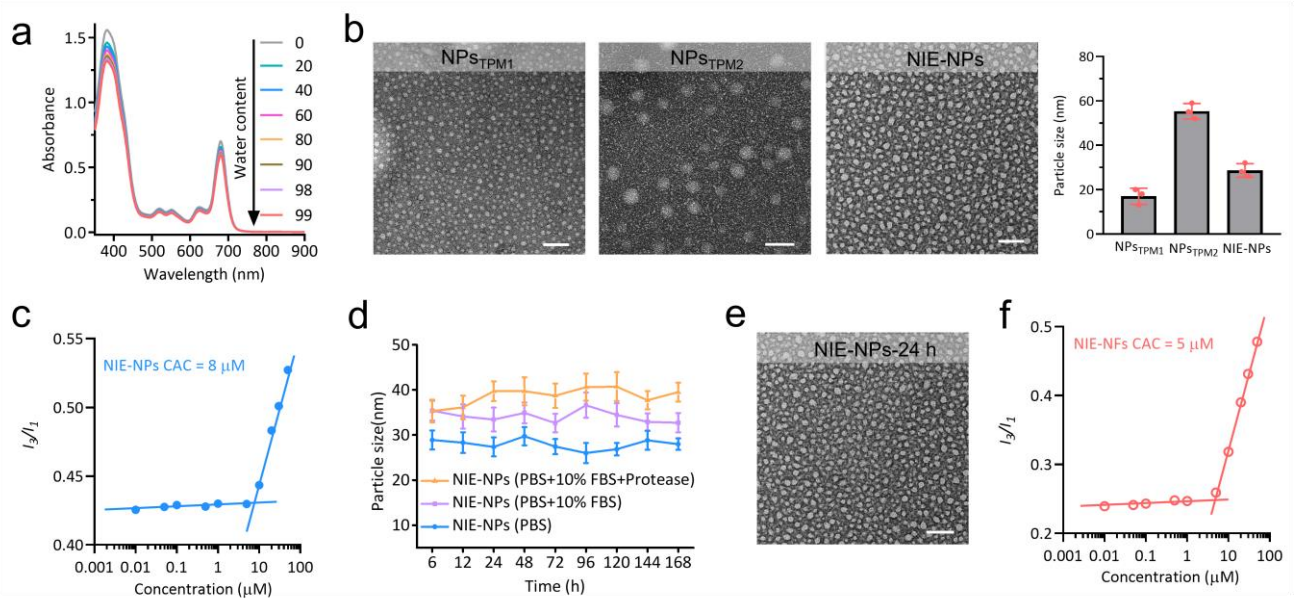

Supplementary Fig. 2. a, Changes in UV imaging of DMSO solution of TPM1 and TPM2 at a 1:1 ratio following the gradual addition of water (from 0 to 99%) forming NIE-NPs. Experiments were repeated three times. **b**, TEM images and size distribution of NPs_{TPM1}, NPs_{TPM1} and NIE-NPs at the H_2O and DMSO ratio of 99:1. Experiments were repeated three times. **c**, The critical aggregation concentration (CAC) of NIE-NPs was measured by using pyrene as a probe. Experiments were repeated three times. **d**, Nanoparticle stability of NIE-NPs in serum and protease (PBS solution of pH 7.4 with/without 10% FBS and protease) at 37 °C was measured by dynamic light scattering. Data are presented as the mean ± s.d., $n = 3$ independent expe riments. **e**, TEM images of NIE-NPs after 24 h in PBS solution. Experiments were repeated three times. **f**, The CAC of NIE-NFs was measured by using pyrene as a probe. Experiments were repeated three times. The scale bar in all TEM images is 100 nm. The concentration of NIE-NPs used in **b**, **d**, **e** was 20 μM.

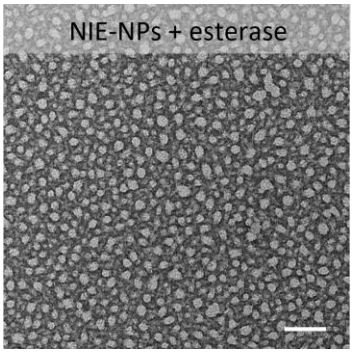

Supplementary Fig. 3. TEM images of NIE-NPs interaction with esterase for 24 h. The concentration of NIE-NPs used in the experiment was 20 μM. The scale bars are 100 nm. Experiments were repeated three times.

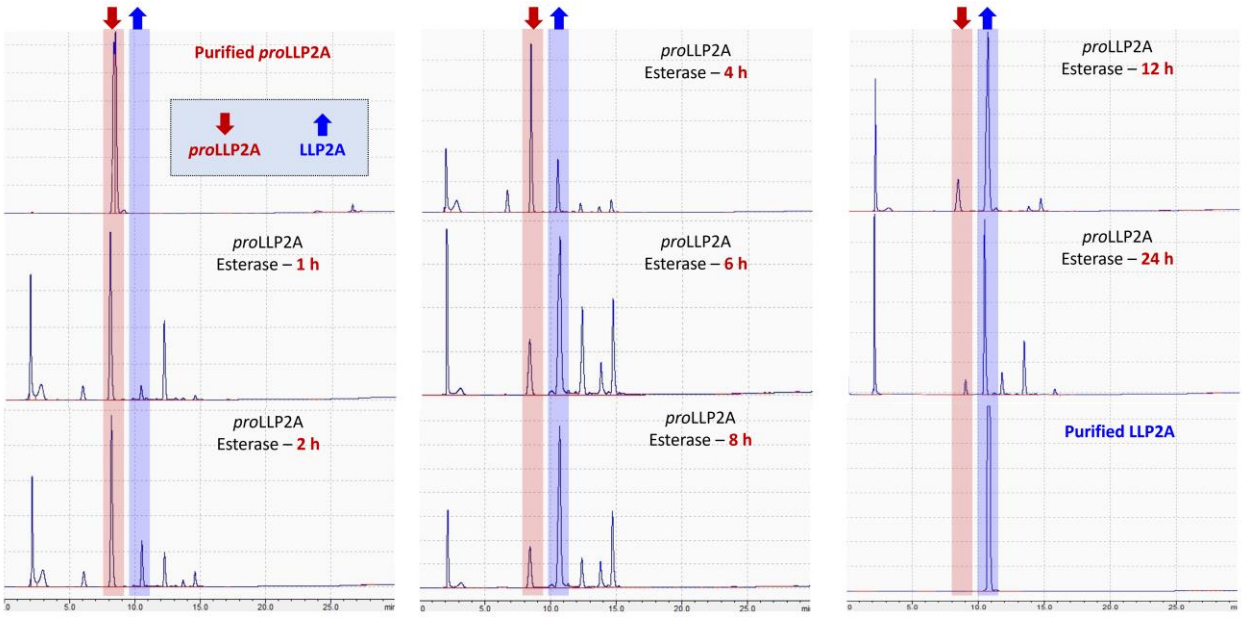

Supplementary Fig. 4. HPLC monitoring on conversion of *pro*LLP2A to LLP2A upon incubation with esterase (porcine liver esterase: 100 U/mL) at 37 °C (pH = 7.4). Experiments were repeated independently three times. LLP2A peak was observed after 1 h incubation of *pro*LLP2A with esterase. By 6 h, the LLP2A peak was higher than that of *pro*LLP2A. By 12 h, the vast majority of *pro*LLP2A had been converted to LLP2A.

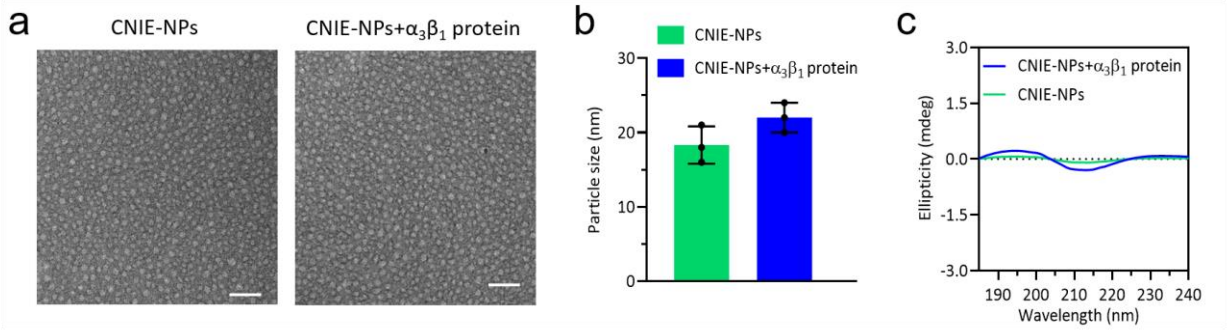

Supplementary Fig. 5. a,b, TEM images (**a**) and particle size (**b**) of initial CNIE-NPs and CNIE-NPs interaction with $\alpha_3\beta_1$ integrin protein for 24 h. The molar ratio of $\alpha_3\beta_1$ integrin protein/peptide ligand was approximately 1:1000. The scale bar is 100 nm. The concentration of CNIE-NPs used in the experiment was 20 μM. Experiments were repeated three times. **c**, Circular dichroism spectra of initial CNIE-NPs and CNIE-NPs interaction with $\alpha_3\beta_1$ integrin protein. Experiments were repeated three times.

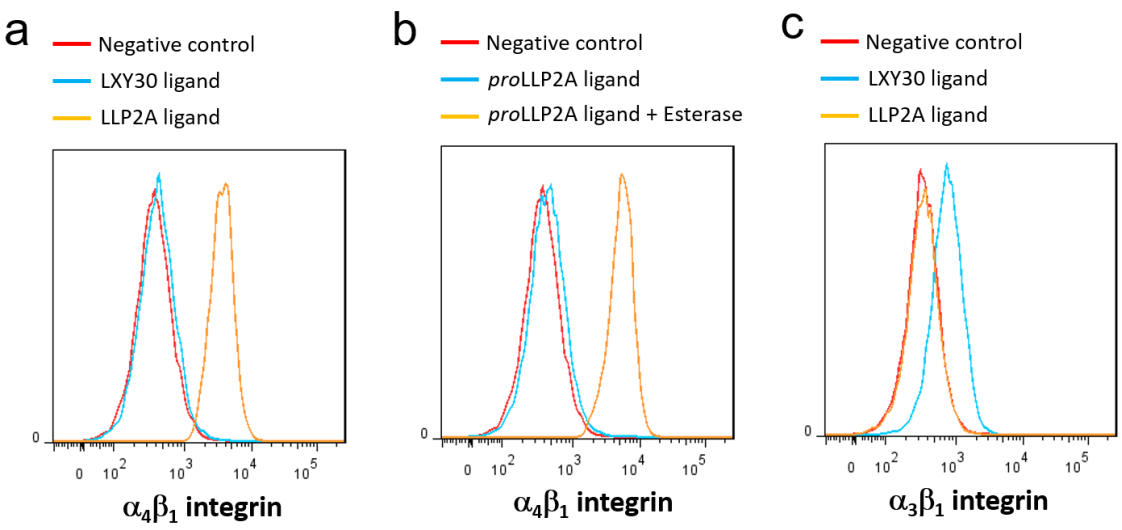

Supplementary Fig. 6. Flow cytometry analysis of ligand binding to integrins. Biotinylated LXY30, LLP2A, *pro*LLP2A and *pro*LLP2A/esterase incubated with $\alpha_3\beta_1$ or $\alpha_4\beta_1$ integrin transfected K562 cells. $3*10^5$ cells incubated with 1 μM biotinylated ligand peptides in binding buffer (1x PBS, 10% FBS, 1 mM Mn^{2+}) for 30 min on ice, after washing with PBS followed by incubation with 1:500 streptavidin-PE (1 mg/mL) for 30 min, then analyzed with flow cytometry.

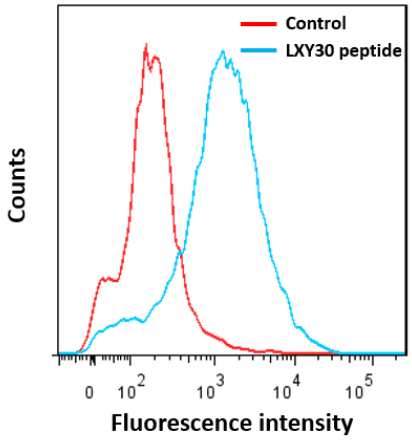

Supplementary Fig. 7. Flow cytometry analysis of LXY30 binding to 4T1 cells. Biotinylated LXY30 peptide (blue curve) and negative control (red curve) incubation with 4T1 cells were analyzed with flow cytometry. Experiments were repeated three times. $3*10^5$ cells incubated with 1 μM biotinylated LXY30 for 30 min on ice, after washing with PBS followed by incubation with 1:500 streptavidin-PE (1mg/mL) for 30min, then run with flow cytometry.

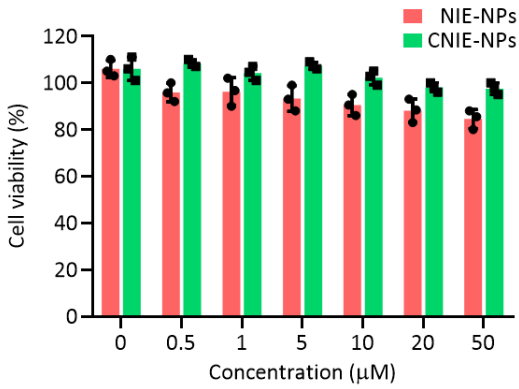

Supplementary Fig. 8. Viability of 4T1 cells after incubation with NIE-NPs and CNIE-NPs at different concentrations for 48 h. Data are presented as mean ± s.d., $n = 3$ independent experiments.

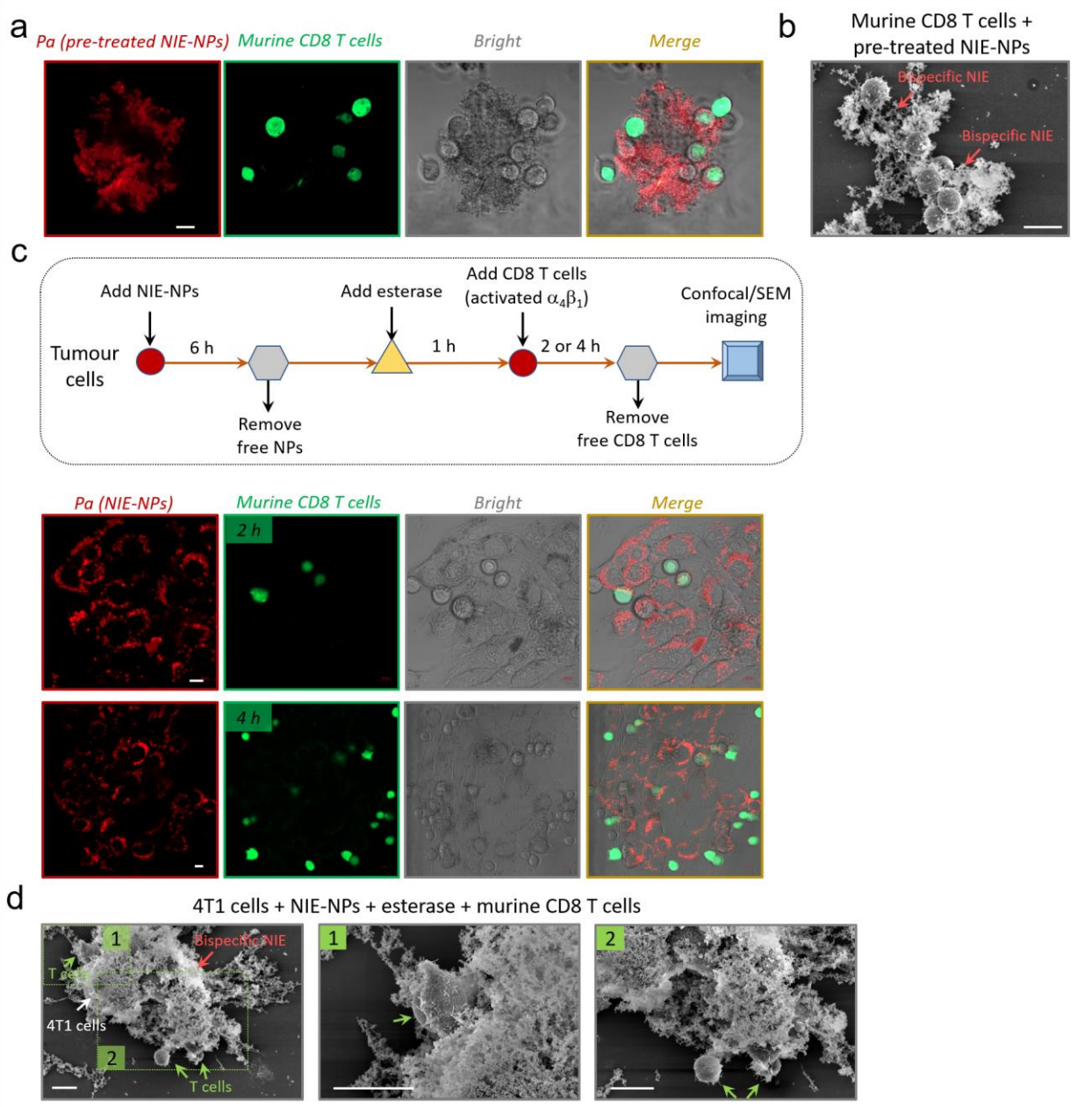

Supplementary Fig. 9. *In vitro* immunoengaging between murine CD8 T cells and target 4T1 breast cancer cells. **a**,**b**, Cellular fluorescence distribution images (**a**) and SEM images (**b**) of murine CD8 T cells (CellTracker™ Green CMFDA Dye Labeled, green color) after incubation with esterase-pretreated NIE-NPs to show NIE around cells. $\alpha_4\beta_1$ integrins on murine CD8 T cells surface were pre-activated by Mn^{2+} (1 mM). Scale bar in **a** and **b** is 10 μm. Experiments were repeated three times. **c**,**d**, Experimental scheme, cellular fluorescence distribution images (**c**) and SEM images (**d**) of NIE-NPs (fluorescent red), after mixing 4T1 tumour cells with murine CD8 T cells ($\alpha_4\beta_1$ integrins were pre-activated by Mn^{2+}). It shows that nanofibrillar networks (bispecific NIE) cover 4T1 tumour cells, which in turn binds CD8 T cells. Longer incubation time, more bound CD8 T cells. Scale bar in **c** and **d** is 10 μm. Experiments were repeated three times.

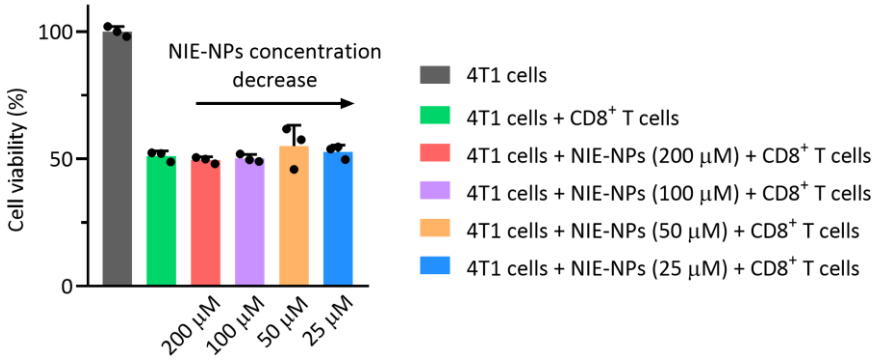

Supplementary Fig. 10. Viability of 4T1 tumour cells after incubation with NIE-NPs at different concentrations (12 h), followed by co-culturing with activated murine CD8 T cells for 24 h. The presence of fibrillar networks and LLP2A ligands on tumour cells surface did not dampen immune synapse formation and killing efficiency of CD8 T cells. CD8 T cells were isolated from spleen using Miltenyi Biotec Dynabeads untouched mouse CD8 isolate Kit and were pre-activated by a cell stimulation cocktail (eBioscience Cell Stimulation Cocktail) for 12 h. Data are presented as mean ± s.d., $n = 3$ independent experiments.

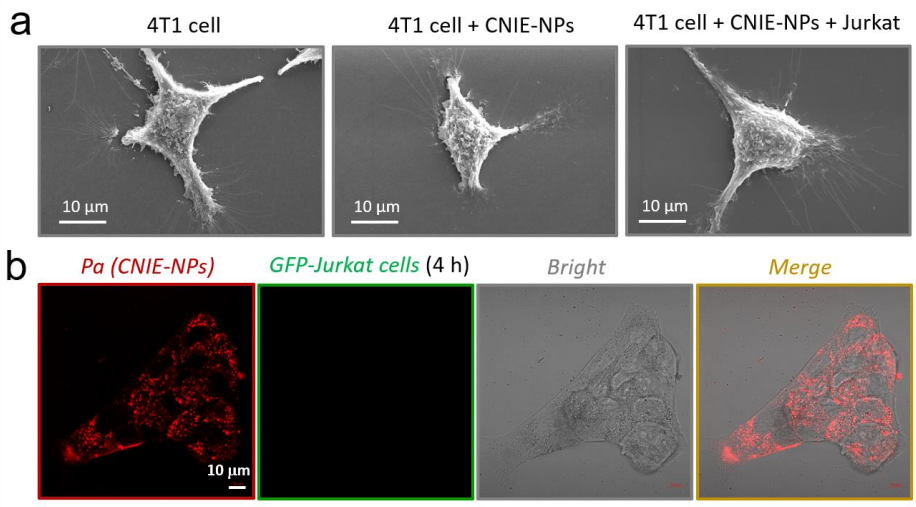

Supplementary Fig. 11. a, Representative SEM images of untreated 4T1 tumour, 4T1 tumour cells treated with negative control CNIE-NPs, 4T1 tumour cells treated with CNIE-NPs and then Jurkat human malignant T-cells for 6 h. Experiments were repeated three times. **b**, Experimental scheme and cellular fluorescence distribution images of CNIE-NPs (fluorescent red), after interaction with 4T1 tumour and GFP-labeled Jurkat cells. It showed that no nanofibrillar structure was found surrounding 4T1 tumour cells; therefore, no bound Jurkat cell (green color) was observed. Experiments were repeated three times.

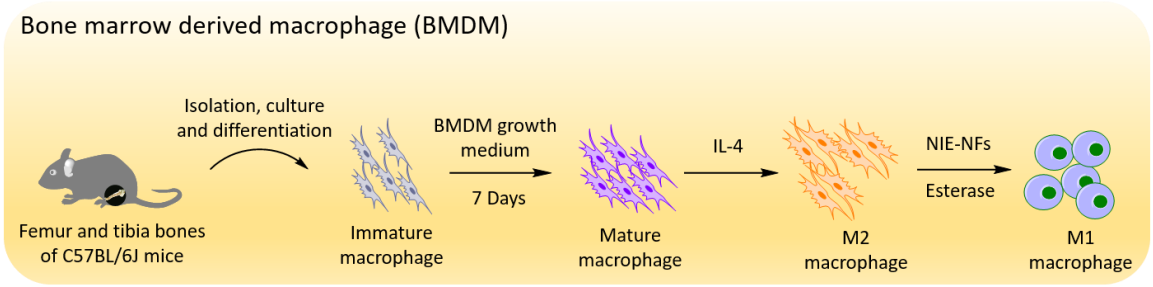

Supplementary Fig. 12. Schematic illustration of the inducing process of M2-like and M1-like tumour-associated macrophage under different conditions.

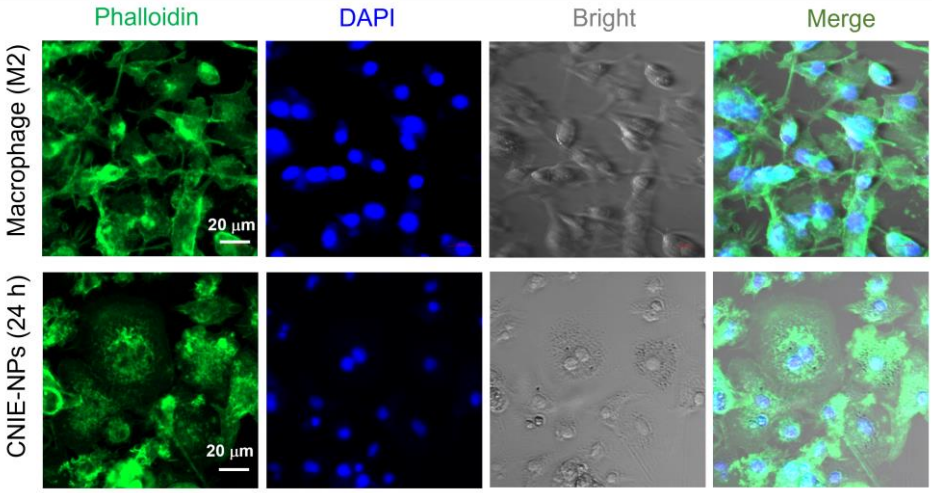

Supplementary Fig. 13. Representative fluorescence images of M2-like murine macrophages treated with CNIE-NPs for 24 h, resulting in conversion of M2 phenotype to M1 phenotype. Experiments were repeated three times.

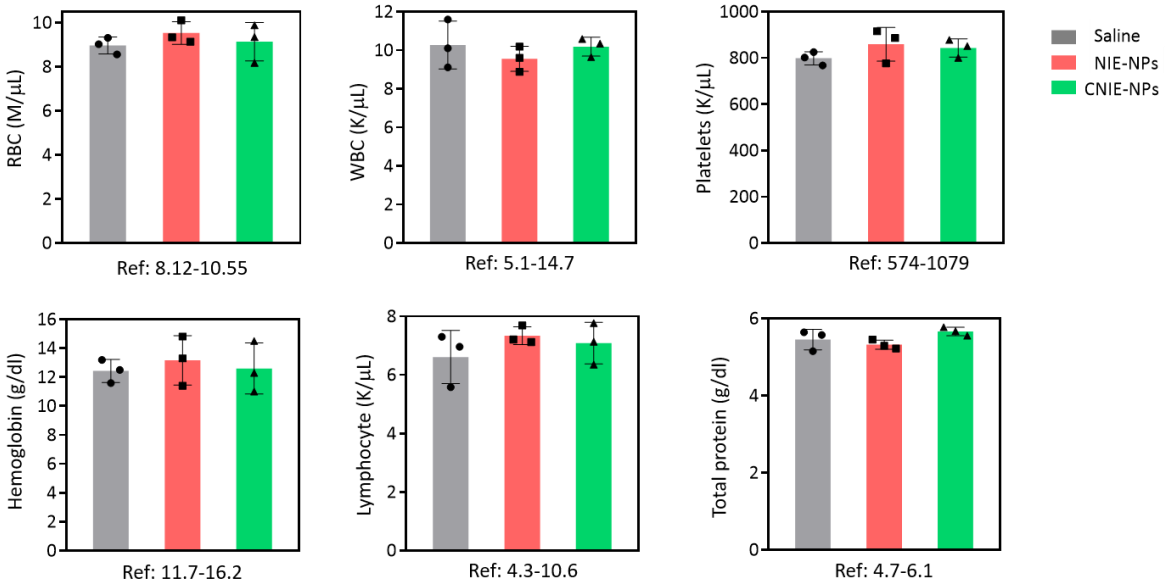

Supplementary Fig. 14. Blood test parameters in terms of red blood cells (RBC), white blood cells (WBC), platelets, hemoglobin, lymphocyte and total protein of healthy Balb/c mice, after 8 q.o.d. intravenous injections of NIE-NPs and CNIE-NPs (13 mg/kg per injection). Data are presented as the mean ± s.d., $n = 3$ independent experiments.

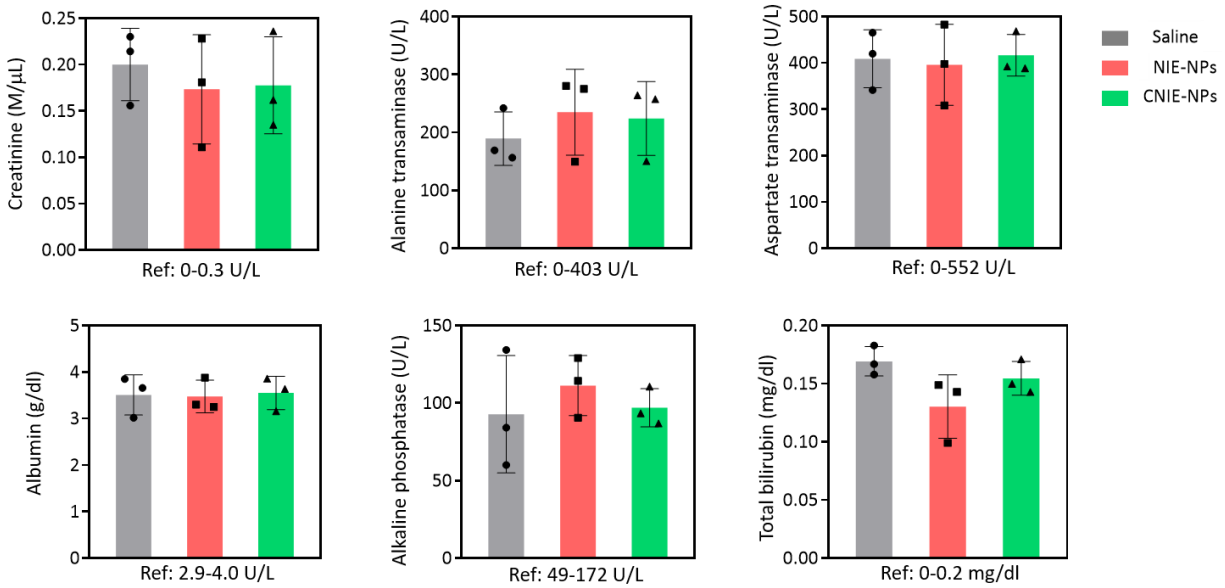

Supplementary Fig. 15. Blood test parameters in terms of liver function creatinine, alanine transaminase, aspartate transaminase, albumin, alkaline phosphatase, total bilirubin of healthy Balb/c mice after 8 q.o.d. intravenous injection of NIE-NPs and CNIE-NPs (13 mg/kg per injection). Data are presented as the mean ± s.d., $n = 3$ independent experiments.

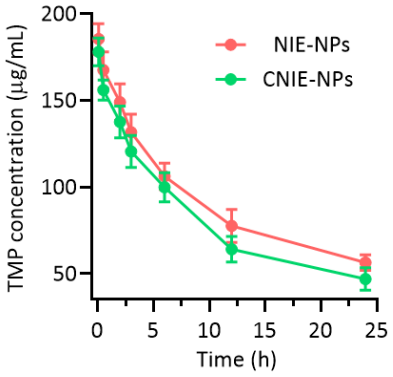

Group	C-max (μg/mL)	AUC	T-half (α)/h	T-half (β)/h
NIE-NPs	193.12	1969.572	2.866	23.1862
CNIE-NPs	186.85	1875.363	2.628	21.9657

Supplementary Fig. 16. *In vivo* blood pharmacokinetics and parameter of NIE-NPs and CNIE-NPs (Data are presented as the mean ± s.d., $n = 3$ independent experiments). The C-max, AUC and $T_{1/2}$ (hours) were calculated by Kinetica 5.0.

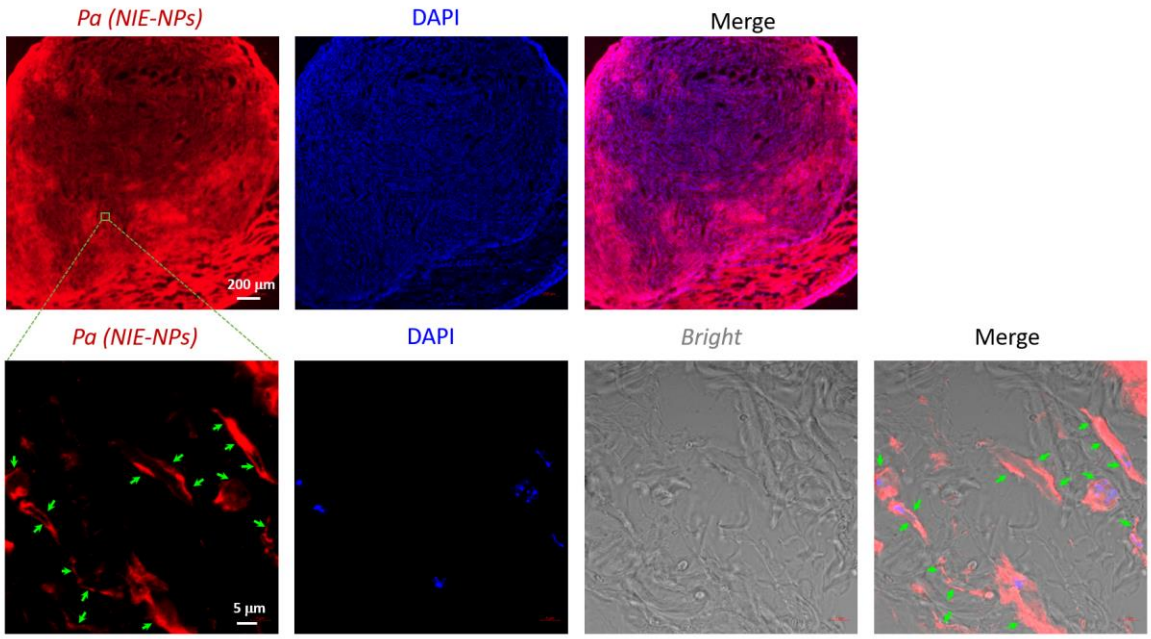

Supplementary Fig. 17. Fluorescence distribution images of the entire excised tumour tissue at 72 h after i.v. injection of NIE-NPs in 4T1 tumour model (red color: *Pa* of NIE-NPs; blue color: DAPI). The NIE-NPs dose used was 13 mg/kg. Experiments were repeated three times. An enlarged detailed outline of the *Pa* fluorescence distribution. The red fluorescence signal from *Pa* was found throughout the entire tumour tissue section, not just at the periphery. And most of the red fluorescence was observed in the extracellular matrix in proximity to the cell membrane, as indicated by the green arrow, indicating that NIE-NPs could transform into fibrillar-structures around the cell membrane *in vivo*.

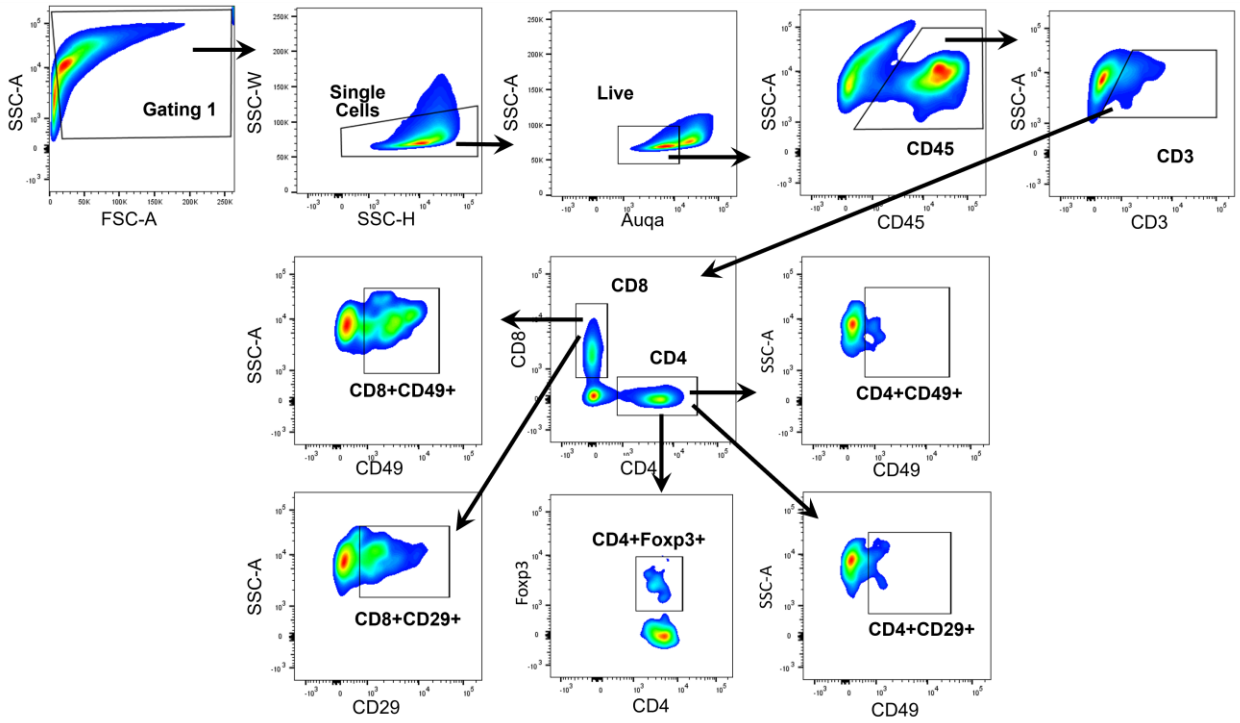

Supplementary Fig. 18. Gating strategies for flow cytometric analysis of CD8 and CD4 T cells, CD49 and CD29 in CD8 T cell and CD4 T cells within the 4T1 tumours tissue.

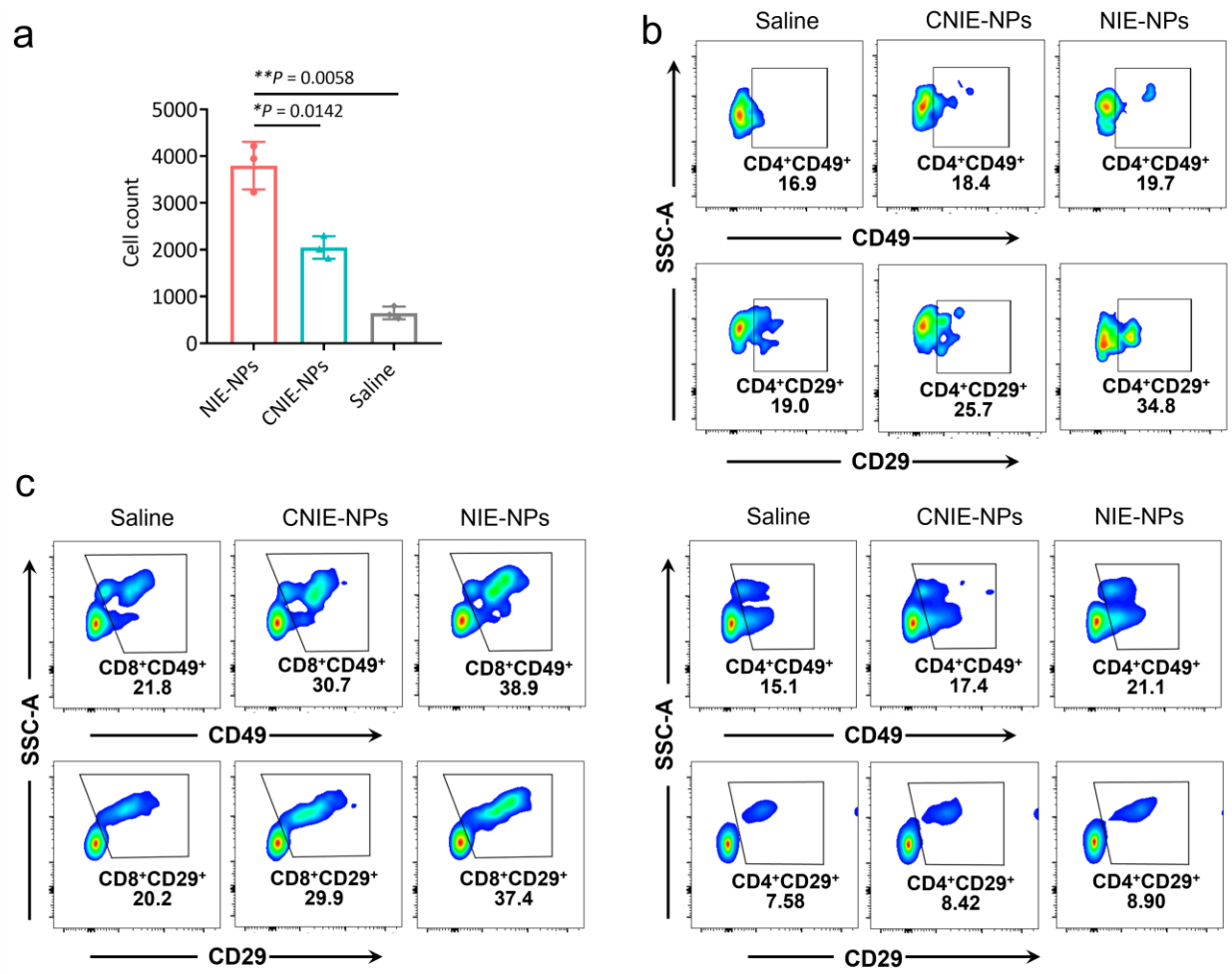

Supplementary Fig. 19. T cell profiling of 4T1 tumours tissue after the mice were treated with saline, CNIE-NPs or NIE-NPs. **a**, Quantification of tumour infiltrating T cells (Fig. 3i). **b**,**c**, Representative flow cytometric analysis images of (**b**) $CD4^+CD49^+$, $CD4^+CD29^+$ T cell in tumour tissue and (**c**) $CD8^+CD49^+$, $CD8^+CD29^+$, $CD4^+CD49^+$ and $CD4^+CD29^+$ in blood circulation.

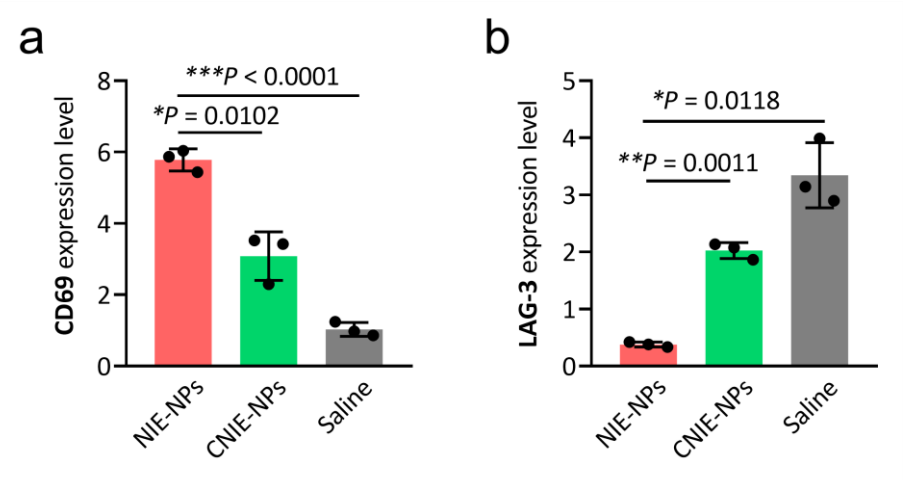

Supplementary Fig. 20. a,b, The expression levels (qPCR assay) of (**a**) CD69 and (**b**) LAG-3 in 4T1 tumours tissue excised from mice 15 days after treatment with NIE-NPs or CNIE-NPs (n = 3; data were mean ± s.d.). Statistical significance was calculated using a two-sided unpaired t test compared to NIE-NPs group; *$P < 0.05$, **$P < 0.01$, ***$P < 0.001$.

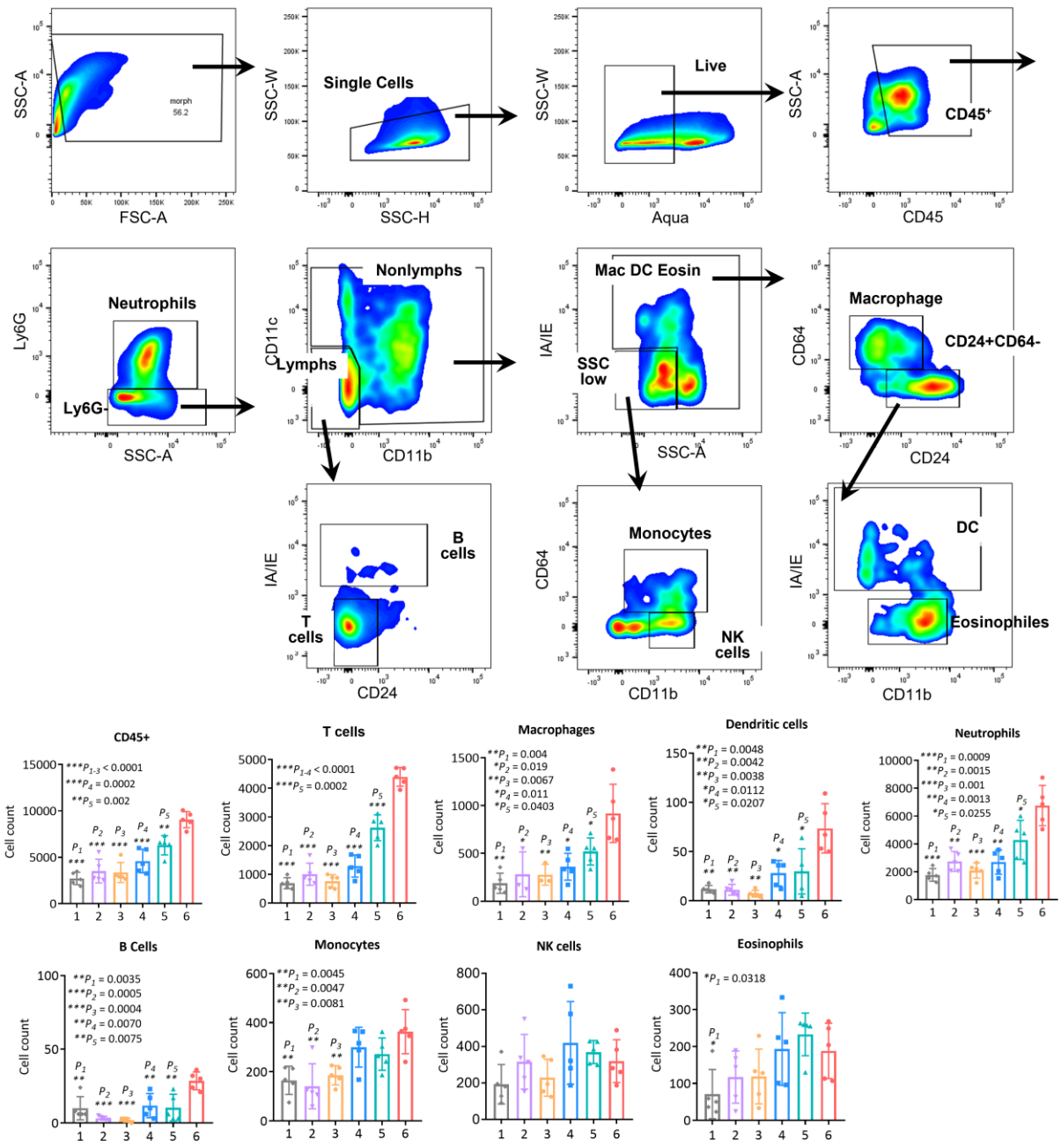

Supplementary Fig. 21. Gating strategies for flow cytometric analysis of immune cells infiltration within the 4T1 tumours tissue and corresponding quantification of CD45+, T cells, macrophages, dendritic cells, neutrophiles, B cells, monocytes, NK cells and eosinophils infiltration within the tumour tissue derived from the indicated treatment groups over 21 days. Statistical significance was calculated using a two-sided unpaired *t* test compared to regimen 6; *$P < 0.05$, **$P < 0.01$, ***$P < 0.001$.

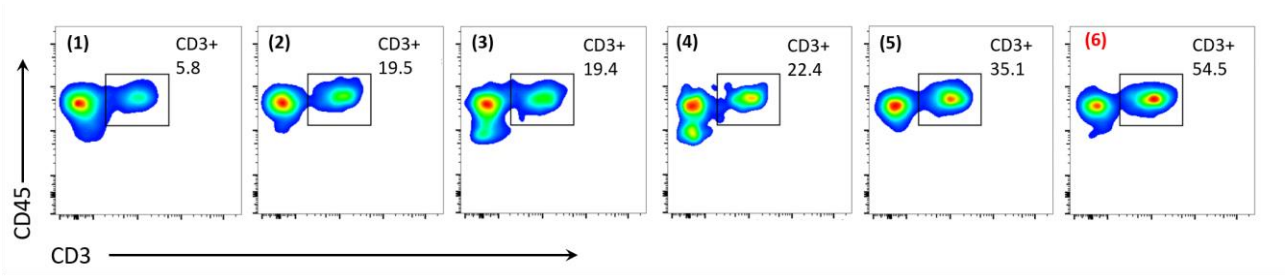

Supplementary Fig. 22. Representative flow cytometric analysis images of $CD45^{+}CD3^{+}$ T cell within the excised 4T1 tumours from mice treated with: (1) Saline; (2) $(EK)_3$-KLVFFK(*Pa*)/$(EK)_3$-KLVFFK(*R848*) (nanoscale R848 due to the bad hydrophilicity of free R848); (3) *pro*LLP2A-KLVFFK(R848) (single monomer); (4) LXY30-KAAGGK(*Pa*)/*pro*LLP2A-KAAGGK(*R848*) (untransformable negative control CNIE-NPs); (5) LXY30-KLVFFK(*Pa*)/*pro*LLP2A-KLVFFK(*Pa*) (fibrillar transformation but absence of R848); (6) LXY30-KLVFFK(*Pa*)/*pro*LLP2A-KLVFFK(*R848*) (NIE-NPs).

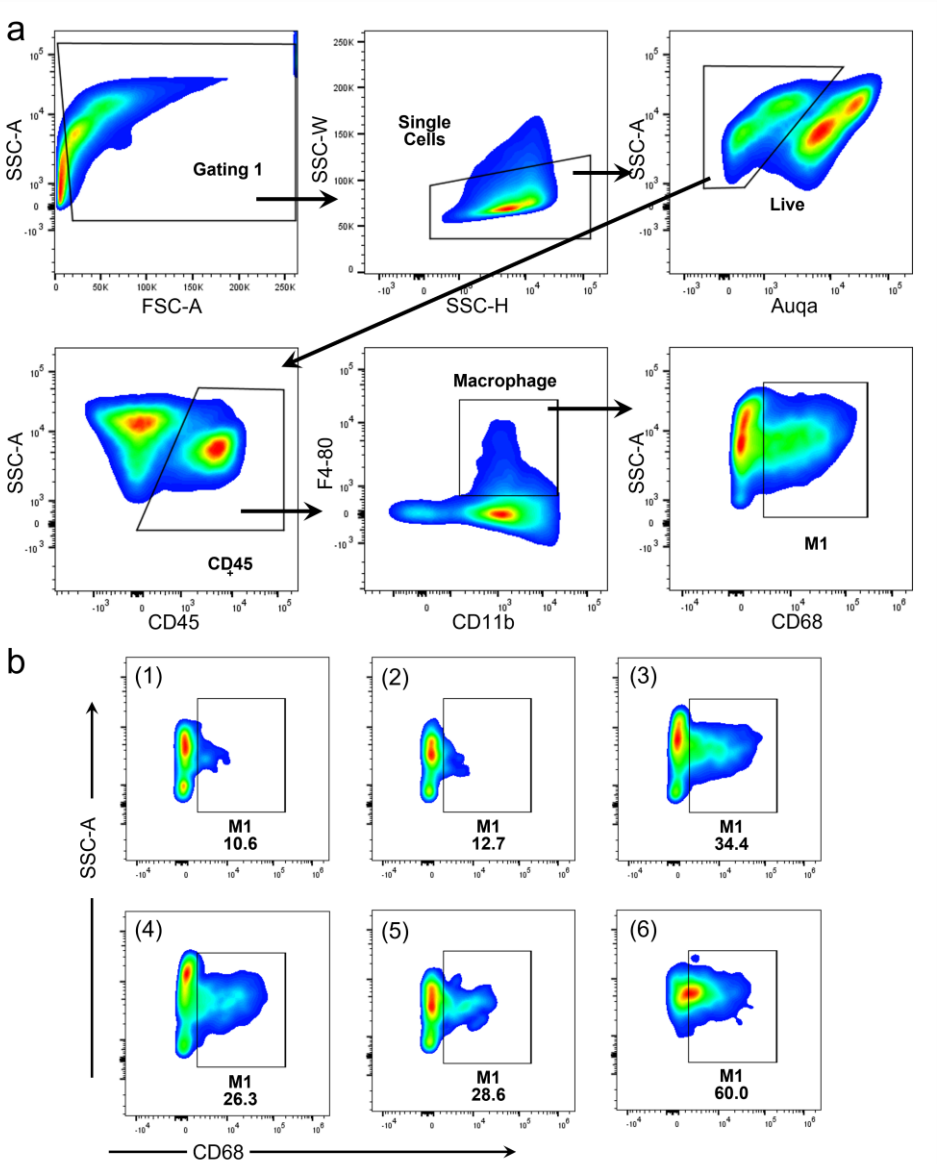

Supplementary Fig. 23. a, Gating strategies for flow cytometric analysis of M1-phenotype macrophage within the 4T1 tumours. **b,** Representative flow cytometric analysis images of M1-phenotype macrophage within the 4T1 tumours excised from treated mice on day 21. (1) Saline; (2) $(EK)_3$-KLVFFK(*Pa*)/$(EK)_3$-KLVFFK(*R848*) (nanoscale R848 due to the bad hydrophilicity of free R848); (3) *pro*LLP2A-KLVFFK(R848) (single monomer); (4) LXY30-KAAGGK(*Pa*)/*pro*LLP2A-KAAGGK(*R848*) (untransformable negative control CNIE-NPs); (5) LXY30-KLVFFK(*Pa*)/*pro*LLP2A-KLVFFK(*Pa*) (fibrillar transformation but absence of R848); (6) LXY30-KLVFFK(*Pa*)/*pro*LLP2A-KLVFFK(*R848*) (NIE-NPs).

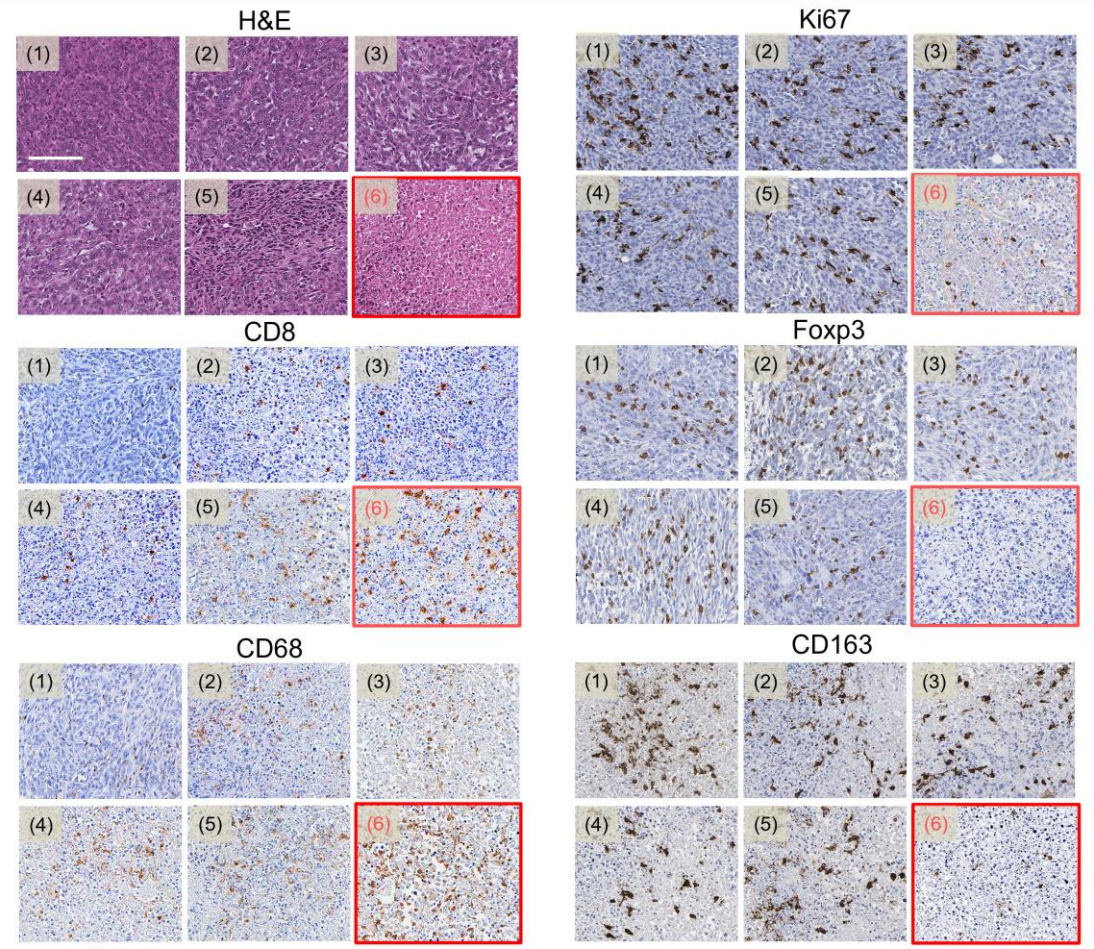

Supplementary Fig. 24. H&E and IHC images of excised tumours tissue. Representative images are shown for the IHC staining of Ki67, T cells (CD8, Foxp3) and macrophage markers (CD68, CD163). Scale bar is 100 μm.

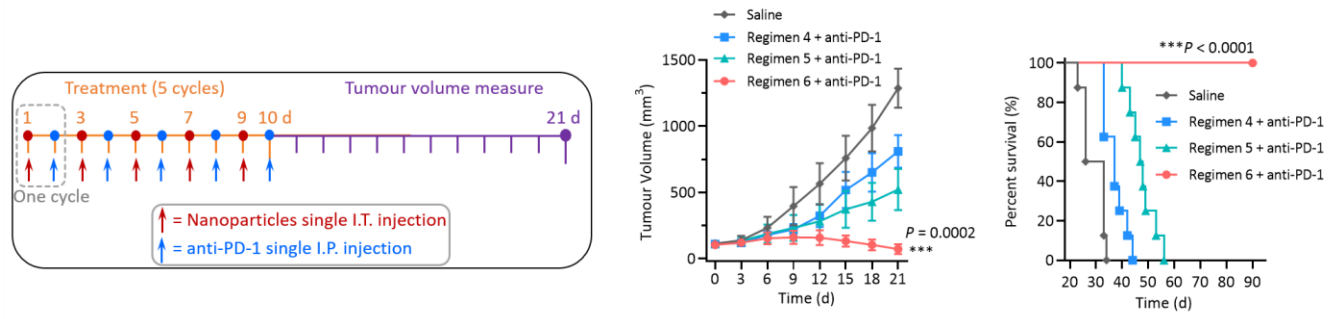

Supplementary Fig. 25. Bispecific NIE (intratumoural injection) combines ICB therapy in mice bearing 4T1 breast tumour. Experimental design: orthotopic tumour inoculation and treatment protocol (4 treatment arms; regimens 4, 5 and 6 are the same as those shown in Fig. 4a). Tumour response in mice bearing orthotopic 4T1 tumour over 21 d of treatment ($n = 8$ per group). Data are presented as mean ± s.d. Cumulative survival of the four treatment groups. Statistical significance was calculated using a two-sided unpaired *t* test compared to Regimen 6 plus anti-PD-1 group; *$P < 0.05$, **$P < 0.01$, ***$P < 0.001$.

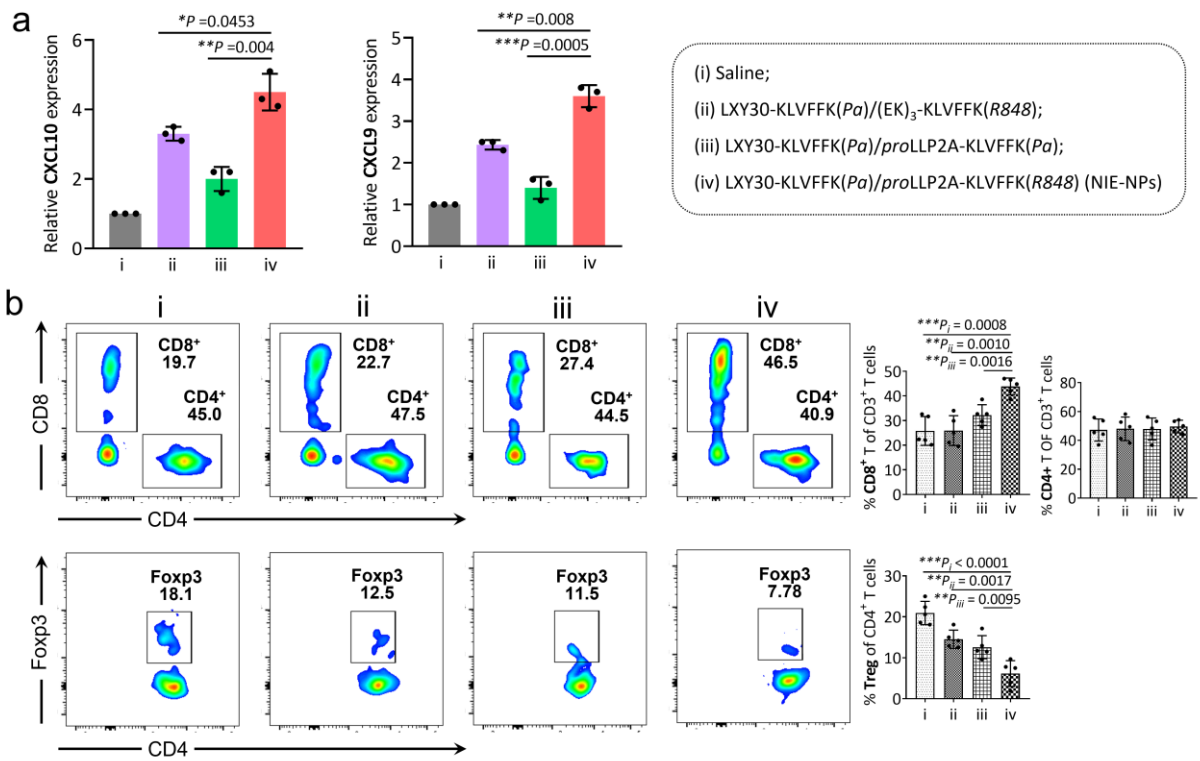

Supplementary Fig. 26. Immune efficacy of bispecific NIE in Balb/c mice bearing 4T1 breast tumour. **a,** The expression of CXCL10 and CXCL9 chemokine on day 7 within the excised tumour tissues of mice after different treatment (n = 3; data were mean ± s.d.). **b**, Representative flow cytometric analysis images and relative quantification of $CD8^+/CD4^+$ and $CD4^+Foxp3^+$ T cell within the 4T1 tumours excised from mice after different treatment at day 15. All treatment regimens were tail vein injected consecutively three times q.o.d. (13 mg/kg each dose, every other day; n = 5; data were mean ± s.d.). Statistical significance was calculated using a two-sided unpaired t test compared to group iv; $^*P < 0.05$, $^{**}P < 0.01$, $^{***}P < 0.001$.

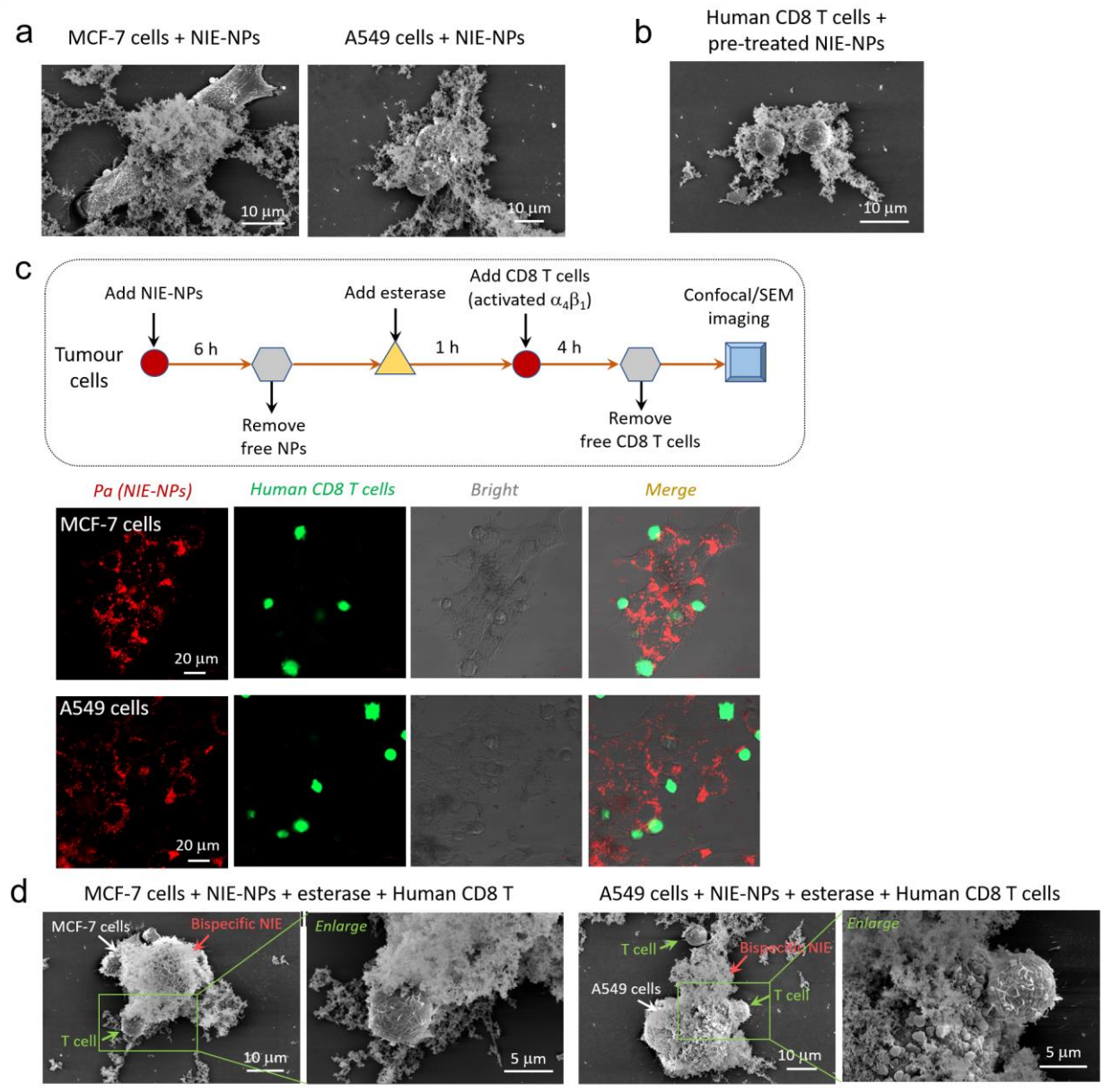

Supplementary Fig. 27. *In vitro* immunoengaging studies using human tumours cells and human CD8 T cells. **a**,**b**, SEM images of (**a**) MCF-7 human breast cancer and A549 human non-small lung cancer cells treated with NIE-NPs and (**b**) human CD8 T cells (CellTracker™ Green CMFDA Dye Labeled, green color) after incubation with esterase-pretreated NIE-NPs to show NIE formed around the cells. $\alpha_4\beta_1$ integrins on human CD8 T cells surface were pre-activated by Mn^{2+} (1 mM). Experiments were repeated three times. Primary peripheral blood mononuclear cells (PBMC) were purchased from ATCC, and human CD8 T cells were isolated using Miltenyi Biotec Dynabeads untouched human CD8 isolate Kit. **c**,**d**, Experimental scheme, cellular fluorescence distribution images (**c**) and SEM images (**d**) of NIE-NPs (fluorescent red), after interaction with MCF-7 or A549 tumour cells and human CD8 T cells ($\alpha_4\beta_1$ integrins were pre-activated by Mn^{2+}). It shows that nanofibrillar networks (bispecific NIE) covers these tumour cells, which in turn binds CD8 T cells. Experiments were repeated three times.